REPORT DOCUMENTATION PAGE

Form Approved
OMB No. 0704-0188

1. REPORT DATE *(DD-MM-YYYY)*	2. REPORT TYPE	3. DATES COVERED *(From - To)*
24-04-2006	Conference Paper POSTPRINT	2005 - 2006

4. TITLE AND SUBTITLE
Innovative Concepts for SSA Applications

5a. CONTRACT NUMBER

5b. GRANT NUMBER

5c. PROGRAM ELEMENT NUMBER

6. AUTHOR(S)
D. H. Huang, D. A. Cardimona, T. Apostolova, P. M. Alsing, W. Glass, and C. D. Castillo

5d. PROJECT NUMBER

5e. TASK NUMBER

5f. WORK UNIT NUMBER

7. PERFORMING ORGANIZATION NAME(S) AND ADDRESS(ES) AND ADDRESS(ES)
Air Force Research Laboratory
Space Vehicles
3550 Aberdeen Ave SE
Kirtland AFB, NM 87117-5776

8. PERFORMING ORGANIZATION REPORT NUMBER
AFRL-VS-PS-TP-2006-1028

9. SPONSORING / MONITORING AGENCY NAME(S) AND ADDRESS(ES)

10. SPONSOR/MONITOR'S ACRONYM(S)

11. SPONSOR/MONITOR'S REPORT NUMBER(S)

12. DISTRIBUTION / AVAILABILITY STATEMENT
Approved for public release; distribution is unlimited. (Clearance #VS06-0143)

13. SUPPLEMENTARY NOTES
Authors' final manuscript, presented at the Space Sensing and Situational Awareness, A NATO Specialist Meeting, 24-25 Apr 06, Maui, Hawaii

14. ABSTRACT
In the Advanced Detectors Research Group of the Air Force Research Laboratory's Space Vehicles Directorate, we explore innovative ways to enhance existing detector technologies and to develop new detector capabilities for future space-based missions, such as space sensing and situational awareness. Space-based sensing needs will be met with the employment of state-of-the-art optoelectronic and photonic techniques that yield high sensitivity, reconfigurable options, high speed, light weight, low power, and radiation hardness. We present some ideas we are presently exploring that address these aspects: (i) amplification or enhancement of weak signals, (ii) continuous tuning of the peak wavelength of a detector response by applying an electric field, and (iii) monolithic solid-state cooling of a detector using optical refrigeration.

15. SUBJECT TERMS
Space-Based Sensing; Detectors; Optoelectronic; Photonic; Space Vehicles

16. SECURITY CLASSIFICATION OF:			17. LIMITATION OF ABSTRACT	18. NUMBER OF PAGES	19a. NAME OF RESPONSIBLE PERSON
a. REPORT	b. ABSTRACT	c. THIS PAGE			Dave A. Cardimona
Unclassified	Unclassified	Unclassified	Unlimited	15	19b. TELEPHONE NUMBER *(include area code)* 505-846-5807

Innovative Concepts for SSA Applications

D. H. Huang, D. A. Cardimona, T. Apostolova, P. M. Alsing, W. Glass, and C. D. Castillo
Air Force Research Laboratory, Space Vehicles Directorate
3550 Aberdeen Ave., S.E., Kirtland AFB, NM 87117-5776
UNITED STATES

danhong.huang@kirtland.af.mil / dave.cardimona@kirtland.af.mil

ABSTRACT

In the Advanced Detectors Research Group of the Air Force Research Laboratory's Space Vehicles Directorate, we explore innovative ways to enhance existing detector technologies and to develop new detector capabilities for future space-based missions, such as space sensing and situational awareness. Space-based sensing needs will be met with the employment of state-of-the-art optoelectronic and photonic techniques that yield high sensitivity, reconfigurable options, high speed, light weight, low power, and radiation hardness. We present some ideas we are presently exploring that address these aspects: (i) amplification or enhancement of weak signals, (ii) continuous tuning of the peak wavelength of a detector response by applying an electric field, and (iii) monolithic solid-state cooling of a detector using optical refrigeration.

1. INTRODUCTION

For Space Situational Awareness (SSA), a satellite would like to detect, track, identify, and determine the status of both cold and hot objects that can be either very near or very far and that could be either sunlit or in eclipse. With this range of requirements, a sensor that has some frequency agility (i.e., is able to detect many different, specific, wavelengths) and has some amplification ability would be ideal. In addition, if detailed information about an unknown object becomes desirable, a sensor system that is extremely small and compact, but that still has all the ideal characteristics of frequency agility and high sensitivity would be a major accomplishment.

Tactical surveillance and reconnaissance missions usually require FPAs operating in atmospheric "windows" where IR transmission is high. The vast majority of applications are in the longwave infrared (LWIR, 7-14μm) window with a small number of applications in the midwave IR (MWIR, 3-7μm) windows. Space-based strategic surveillance and situational awareness missions call for FPAs operating in many of the same spectral bands as their tactical counterparts, however, mission and space environment constraints usually make even the most outstanding tactical FPAs unacceptable for space missions. Space surveillance and SSA often requires observation of extremely faint objects against dark backgrounds. These missions call for LWIR or very longwave IR (VLWIR, 14-30μm) FPAs to detect cold objects or to increase the detection range. Often, these distant objects form 'images' within only one or two pixels – thus requiring extremely uniform arrays for tracking purposes. The dark backgrounds place very stringent requirements on the noise characteristics of the sensor system, resulting in FPAs that must be cooled rather substantially, and the limited

satellite power restricts the power consumption allowed by the cryogenic subsystem. To lower the launch costs, the volume and weight of the sensor should be minimal, and for operation in the harsh environment of space, the sensor must be immune to the radiation found there (protons, gamma rays, etc.). Finally, if we desire to determine the status of an unknown object (is it alive or dead, what is its function, etc.), an SSA sensor system should be able to be placed on a small, maneuverable satellite and should be able to detect a wide range of wavelengths (visible for optical observation, IR for thermal characteristics, THz for power generation, etc.).

We are investigating the possibilities of creating a multifunctional, monolithically-integrated sensor system. We envision a sensor in which each individual pixel has a protection layer, an amplification layer, a detection layer, a solid-state cooling layer; all monolithically grown with the readout electronics and some on-chip data processing capability. This should result in a self-protecting sensor with improved detection efficiency, increased functionality, reduced volume and weight, increased reliability, and reduced cost (both for fabrication and for final launch). In this paper we describe our ideas for optical signal amplification, frequency agile detection, and on-chip solid-state cooling.

2. OPTICAL SIGNAL AMPLIFICATION

2.1. Quantum Interference

The field of nanoscience includes the study of synthetic nanostructures created by nanometer-scale building blocks. What makes synthetic nanostructures so attractive is that electrons no longer flow through conductors like rivers. On this scale, the wave nature of an electron is observable, such as an electron tunneling through a thin insulating layer or the self-selection of the polarization of an optical response. These features can often be exploited for creating electronic and electro-optic devices and components. A multiple-quantum-well (MQW) structure is one example of a synthetic nanostructure built by sandwiching a 5-10 nm layer of a narrower bandgap semiconductor material (e.g., GaAs) between layers of a similar material with a wider bandgap (e.g., AlGaAs) (thus forming a “well” surrounded by “barriers” in energy-position space) in a repeated pattern. The sharp interface between the well and barrier materials and the nanometer scale of the well thickness provide a strong confinement to electrons in the direction perpendicular to the well layers. As a result, electron motion in the direction of confinement becomes quantized and subband energy levels are formed. The number of confined energy levels and their separation depend on the well and barrier material and dimensions. In principle, the energy separation can be tailored to respond to incident light with wavelengths ranging from MWIR to VLWIR, and under special conditions even longer (to mm-wave).

Quantum well infrared photodetectors (QWIPs), which employ the unique optical and transport characteristics of MQWs, are based on intersubband absorption in III-V semiconductor MQW heterostructures, and have been rapidly developed to the point where they are now extremely attractive for a growing number of sensor applications. These detectors lend themselves exceptionally well to bandgap engineering of the wavelength response. QWIPs exhibit very high uniformity and their fabrication is relatively cheap when compared with mercury-cadmium-telluride and silicon-IBC detectors. QWIPs can be engineered for any cutoff wavelength of interest between 4 and 25 microns. Also, large format QWIP arrays are easily attainable (640 x 480 has been demonstrated in a camera, and 4096 x 4096 has been fabricated). These devices can be tailor-made to detect long wavelength IR radiation (20μm or longer), and they present the exciting possibility of multi-wavelength detection within a single pixel. MWIR/MWIR, MWIR/LWIR and LWIR/VLWIR QWIP arrays have been demonstrated. Due to the quantum confinement of the electrons within QWIPs, they also have the unique capability that their peak wavelength response can be tuned with an applied bias voltage.

Although considerable progress has been made in QWIPs, their relatively low quantum efficiencies constitute their greatest problem for space-based applications. We are investigating an innovative concept for creating an inversion within the quantum wells that will amplify an incoming infrared signal before sending it into a detector. The proposed device structure will be perfect for monolithic integration with a QWIP or other IR detector. (See Figs. 1 and 2.)

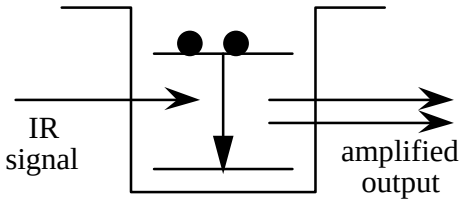

Figure 1: Create a population inversion in a quantum well so that an input photon will stimulate the emission of a duplicate photon.

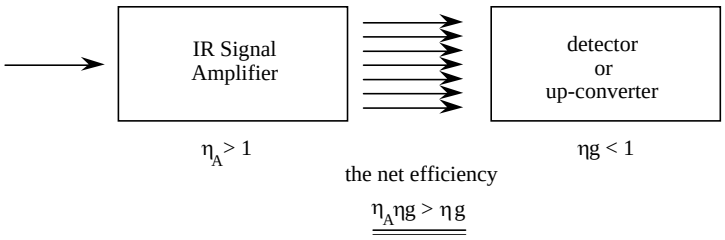

Figure 2: Put IR amplifier in front of any IR device that needs its efficiency improved.

The prerequisite for creating an IR amplifier in a semiconductor quantum well heterostructure is to obtain a population inversion between the states within the quantum well at which the infrared transition is to occur. The idea we describe here extends the ground-breaking work in field-induced transparency in atoms [1] into the realm of semiconductor QWIPs [2]. The original research performed in atomic physics basically discovered that if you had a three-level atomic system with two excited states each coupled by a dipole moment to a single ground state, you could tune an applied pump field in such a way as to trap population in the excited states (see Fig. 3).

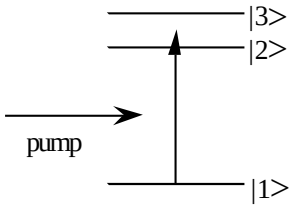

Figure 3: Three-level system for trapping population in the excited states.

The coherent excitation of the two closely-spaced upper states creates a quantum mechanical interference between the 2-to-1 transition and the 3-to-1 transition, resulting in a net zero dipole moment for the system. The population then becomes trapped in the excited states, since with a zero dipole moment, the applied field can no longer interact with the system. The system then becomes “transparent” to the applied field. (S. E.

Harris studied a related phenomenon and called it “electromagnetically-induced transparency” or EIT [3].)

To extend this idea of population trapping in excited states due to quantum interference into the realm of semiconductor materials, we need to devise a three-level system that can be bandgap engineered. One of the exciting things about semiconductor heterostructures is their flexibility in the types of quantum-confined structures that can be created with them. If we sandwich GaAs material between two layers of AlGaAs, the energy band structure becomes shaped like a quantum well, with electrons being trapped energetically within the GaAs well. If the AlGaAs barrier layer is only about 4 or 5 nm thick, and then another GaAs/AlGaAs well/barrier pair are grown, electrons within the two GaAs well layers can interact with each other by tunneling through the barrier layer. When that happens, degenerate energy levels within the two well layers interact and quantum mechanically split into a doublet structure (see Fig. 4).

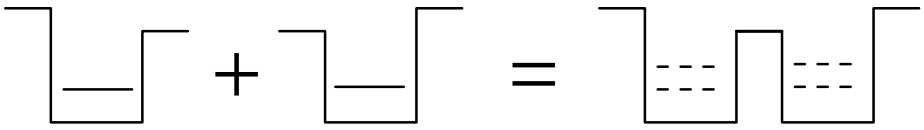

Figure 4: Doublet structure formation due to tunneling interaction between two quantum wells.

With this in mind, we believe that a possible IR amplifier structure should therefore consist of a shallow well with a single bound state separated by a narrow barrier from a deeper well having two bound states, the higher energy state being degenerate with the single state in the other well. The two degenerate states will quantum-mechanically interact through the barrier and split into a doublet state. A coherent pump field at the frequency that will couple the valence band hole state with the doublet of the shallow well induces the transparency effect. This sets up an inversion between the excited state doublet in the deeper well and that well’s ground state. An infrared photon at the frequency of the transition between the states of the deeper well should now see amplification. (See Fig. 5.)

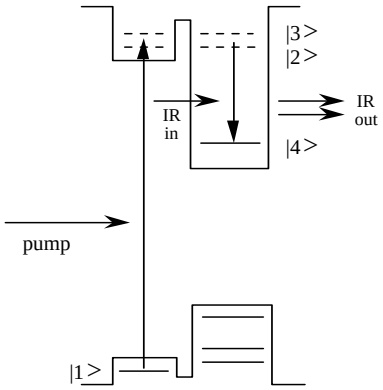

Figure 5: The semiconductor quantum well structure that is predicted to replicate the coherent population trapping found in the three-level atomic system and allow for an inversion to occur.

A stack of these structures should produce a cascading multiplication of the incident IR photon. This amplified signal can then be sent into a monolithically-grown detector structure. (See Fig. 6.)

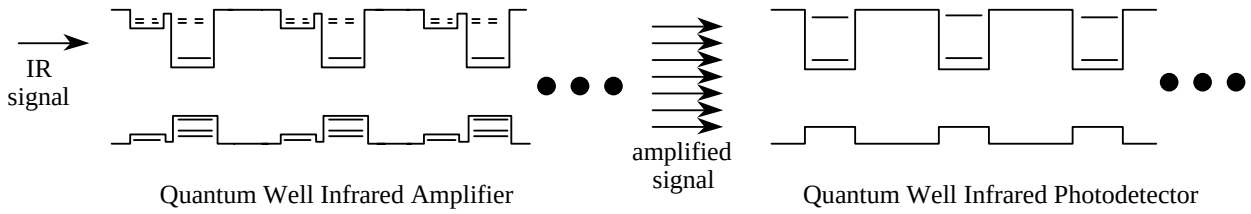

Figure 6: Representation of growth of amplifier quantum well layers monolithically with the QWIP layers.

2.2 Plasmonics

A plasmon is a quantized electron density wave in a conducting material. Bulk plasmons are longitudinal excitations, whereas surface plasmons (SPs) can have both longitudinal and transverse components. Light of frequency below the frequency of the plasmon for that material (the plasma frequency) is reflected, while light above the plasma frequency is transmitted. SPs on a plane surface are non-radiative electromagnetic modes, that is, they cannot be generated directly by light nor can they decay spontaneously into photons. However, if the surface is rough, or is patterned in some way, light around the plasma frequency couples strongly with the surface plasmons, creating what is called a polariton, or a surface plasmon polariton (SPP). An SPP is a localized, coupled electromagnetic field/charge-density oscillation, which may propagate along an interface between two media. SPs play a role in surface-enhanced Raman scattering. When they couple to the incident light, they can actually enhance the electric field in the near field (the evanescent field).

Very recently, Ebbesen *et al.* [4] have reported an enhanced optical transmission seen in arrays of subwavelength cylindrical holes in metallic films. These enhanced optical transmissions are believed to be related to light coupling to SPPs in non-structured or structured metallic films. For a very thin metallic film with thickness less than both the incident wavelength and the absorption length of the metal, only one two-dimensional (2D) gapless plasmon mode exists. For a thick metallic film, on the other hand, a 3D plasmon mode with a gap can exist, in addition to the existence of SPP modes. For semi-infinite metals, two surface-plasmon modes can exist.

We have studied a unique structure composed of a half-space of air and a doped semi-infinite GaAs bulk covered by a heavily-doped InAs conducting interface sheet, from which the physics behind the resonant coupling between 3D and 2D plasma-wave excitations and the effect of evanescent modes can be explored. The reasons for choosing the doped InAs instead of a metal are: (i) so that the doping density can be varied and (ii) the homogeneous broadening in InAs is much smaller than that in a metal, which ensures the resonant coupling between 3D and 2D plasma-wave excitations. The inclusion of a doped GaAs bulk allows for both surface and 3D plasma waves [5] in addition to the 2D plasma wave existing in the InAs conducting sheet. The presence of both 3D and 2D plasma waves enables the longitudinal and transverse electromagnetic oscillations to couple in directions both perpendicular and parallel to the sheet. We have developed a spatially-nonlocal dynamic theory in order to determine the transmissivity of an electromagnetic wave incident on our proposed structure [6]. With this structure, we explored the physics behind the resonant coupling between 3D and 2D plasma-wave excitations due to induced current and material polarization within the sheet and the effect of evanescent modes. We also investigated effects due to strong interactions between excited carriers and incident photons.

In addition to several effects due to resonant coupling between 2D and 3D plasma-wave excitations, we predict an evanescent-mode-enhanced optical transmissivity by the doped semi-infinite GaAs bulk (see Fig. 7).

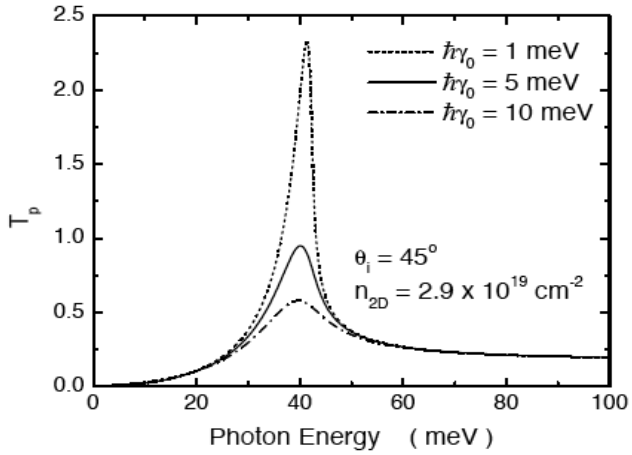

Figure 7: This graph shows how the transmission is enhanced in the near field as the plasmon lifetime decreases (i.e., as the amount of electron scattering increases).

The evanescent-mode-induced near-field enhancement can be used to increase the sensitivity of quantum detectors buried just below the bulk surface, since their photoresponse depends only on the *E*-field and not on the *H*-field component (see Fig. 8).

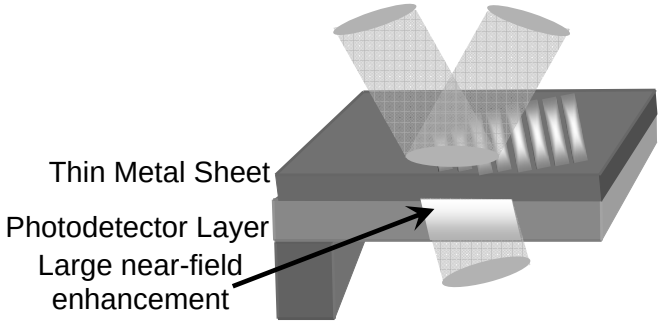

Figure 8: This is a representation of a concept for amplifying an incoming optical signal in a layer of detector material, using plasmonic interactions to enhance the near-field transmission through a metal film.

The evanescent-mode-induced enhancement does not violate energy conservation since these modes do not carry any net energy. For the near-field angular distribution, the presence of the InAs conducting sheet on top of the doped GaAs bulk enhances the transmitted *E*-field for *s* polarization but leaves the transmitted *E*-field almost unchanged for *p* polarization. The enhancement of the transmitted *E*-field in our structure is predicted to be as large as ten times greater than that obtained with an InAs conducting sheet on an undoped GaAs bulk.

2.3 Photonic Crystals

Photonic bandgap (PBG) materials (also called photonic crystals, or PhCs) are to electromagnetic fields as semiconductor materials are to electrons. Just as semiconductor materials have forbidden energy bandgaps

due to the periodic arrangement of many atoms, a material with periodic variations in the dielectric constant can lead to a gap in the frequencies of electromagnetic radiation allowed to exist and propagate in the structured material. The principle of the gap formation is the same in both: Bragg-like diffraction of the electron waves off the atoms in the semiconductor lattice and Bragg scattering of optical waves by the dielectric interfaces in the periodically-structured material. Periodic variations in the dielectric constant in one dimension (1D), e.g. planar layers, lead to a PBG for light incident on the material in that dimension (see Fig. 9a).

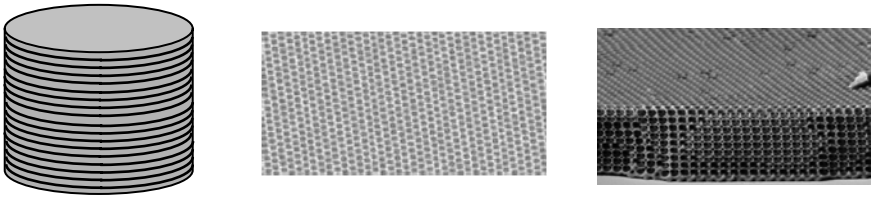

1D Photonic Crystal (a) | 2D Photonic Crystal (b) | 3D Photonic Crystal (c)

Figure 9: (a) 1D photonic crystal, periodic in one dimension – stack of alternating layers of low and high index of refraction materials. (b) 2D photonic crystal, periodic in two dimensions – holes punched in planar material. (c) 3D photonic crystal, periodic in three dimensions – three-dimensional lattice of holes in a bulk material of high index.

If the variations are in two dimensions (2D), e.g. holes punched in a planar material, then the PBG will manifest for light incident within the plane of the holes (see Fig. 9b). A 3D PhC will consist of dielectric variations in all dimensions, and will produce a PBG for light incident from any direction (see Fig. 9c).

Once a material with a PBG has been created, it is possible to introduce a defect into the material (by subtracting or adding dielectric material at one spot – see Fig. 10 for a 2D example), analogous to acceptor or donor defects in semiconductors.

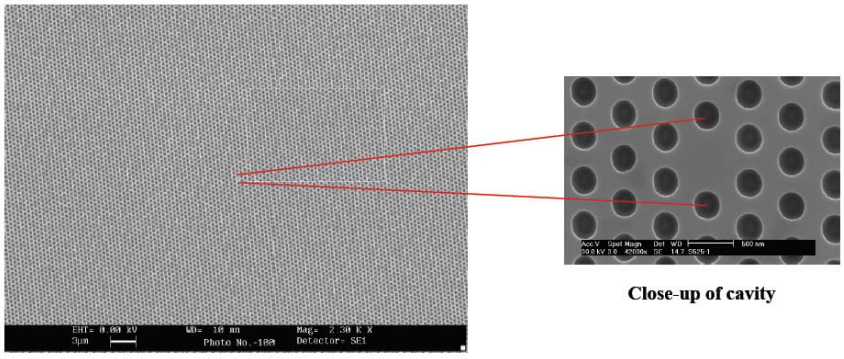

Figure 10: A 2D photonic crystal fabricated as a regular periodic array of air holes in a high index of refraction material. A 2D cavity is formed by creating a defect, i.e. the absence of a hole.

Similar to how these semiconductor defects introduce energy levels into the forbidden bandgap, the defect in a PhC can be designed with any frequency in the PBG, thereby allowing electromagnetic radiation at that frequency to exist and propagate in the crystal. Because the photonic defect is surrounded by a material with a PBG, the field should experience little or no loss, similar to being in a high-Q cavity. Thus, defects within

PBG crystals can be considered microcavities. These microcavities can have extremely long lifetimes, at the same time that they have very small modal volumes. These unique features enable a range of novel applications that take advantage of the emerging field of nonlinear photonic crystals [7]. PhC microcavities have properties that greatly enhance optical nonlinear effects, and show great promise for producing devices for all-optical signal processing. Lengths of these devices can be smaller than the wavelength of light, they can operate with only milliwatts of power, and they can be faster than 10ps. If the enhancement properties of these PhC microcavities are combined with materials that have extremely large nonlinear responses, then devices of unprecedented optical nonlinear response can be created. In addition, placing a highly dispersive material within one of these cavities will greatly enhance its lifetime. It turns out that materials that can exhibit the phenomenon of EIT will manifest both extremely large nonlinear responses as well as extremely strong dispersion.

We will investigate EIT in semiconductor quantum dots inside photonic crystal cavities. The simplest form of PhC can be created using multilayer films that consist of periodically arranged dielectric materials with alternating high and low indices of refraction. If the thickness of each layer satisfies the Bragg condition, then a well-defined gap in the range of frequencies allowed will form in one dimension. If we further enclose this layered structure with a cylindrical metal mirror through a metal diffusion process in the growth direction, the cavity confinement can be increased, allowing the light to be trapped within the cavity. The ease of fabrication of such structures, and the ease with which a good many quantum dots can be placed on planes between such periodic layers, make these 1D PhCs extremely useful for the study of cavity QED and quantum optics in PBG materials (see Fig. 11).

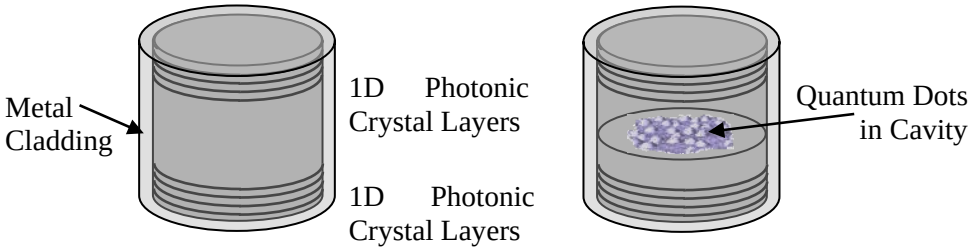

Figure 11: 1D photonic crystal with cavity (left) and with quantum dots embedded in cavity (right).

To obtain higher Q cavities, we will investigate defect cavities in 2D PhCs (see Fig. 12). The 2D PhC cavity can be formed by creating a point defect in the 2D PhC sandwiched between two metal mirrors (cladding layers). The quantum dots inside the 2D PhC cavity can be fabricated using a selective etching technique. The main technical drawback to this geometry will be the small number of quantum dots that will fit into a 2D microcavity. Perhaps an array of such cavities within the 2D PhC will be of more practical use.

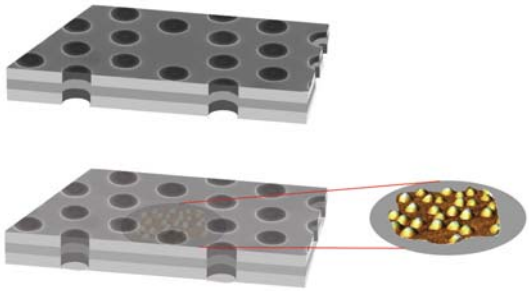

Figure 12: 2D photonic crystal cavity with embedded quantum dots.

For the highest Q-factor, we will want to investigate a full 3D PhC, which is much more difficult to fabricate. The 3D PhC cavity can be formed by creating a point defect inside it. Colloidal quantum dots might then be fed into the hollow space at the center of the 3D PhC through the Si-wafer bonding technique (see Fig. 13).

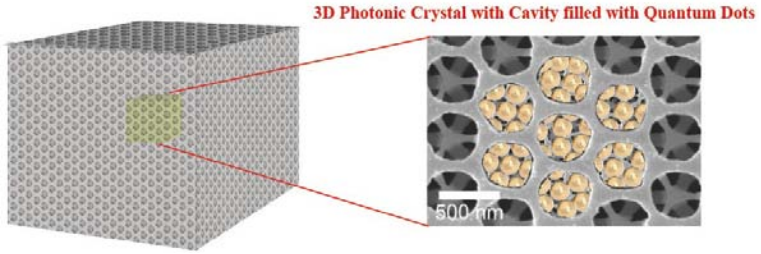

Figure 13: 3D photonic crystal cavity is formed by creating a point defect within the crystal and filling the resulting hollowed space with colloidal quantum dots.

3. FREQUENCY AGILITY

One sensor feature that enables object discrimination and identification is the ability to determine the exact spectral signature of the object. Currently, this feature is implemented using spectral filters and multiple FPAs, each with its own set of optical elements. Bandgap-engineered QWIPs, as well as quantum dot infrared photodetectors (QDIPs) have been shown to exhibit a voltage-tuning capability where the spectral response of a single device can be "tuned" when a bias voltage applied across the growth layers (parallel to the growth direction) is varied. This voltage tuning is produced by the quantum-confined Stark Effect – the shifting of quantized energy levels due to an applied electric field. Voltage tunability can be used to determine the exact spectral signature of the target, without the use of spectral filters or multiple FPA channels. This could result in a significant reduction in the complexity, cost, and weight of the sensor.

The above so-called vertical biasing is not the only possibility. We can also apply a bias field laterally across the pixel, parallel to the plane of the quantum wells (perpendicular to the growth direction). In this case, we first design an asymmetric double quantum well (DQW) structure with a thin middle barrier between the two wells. In this asymmetric DQW structure, a narrow well doped with electrons contains a ground state and an excited state, while a step-lifted wide undoped well contains only one state, resonant with the excited state in the narrow well (see Fig. 14). The most important innovation of this DQW structure is that the two quantum wells can be independently biased laterally from the sides of the pixel, so that planar transport instead of vertical transport can occur in the individual wells and can be controlled independently. The step up to the wide well will be used to reduce the dark current when it is biased laterally. When the electrons in the narrow quantum well absorb a photon, they can transit to the upper excited state in the same well and then rapidly move into the wide well through a resonant tunneling process due to the thin barrier between these two wells. Consequently, the electrons in the wide well will be swept to the collector region when the lateral bias is applied to this well. Because the photo-excited electrons are driven by the lateral bias in one of the quantum wells, a unit optical gain is expected due to the lack of carrier capture processes in the transport (compared to 20% or less in vertically-biased QWIPs). In addition, the bias voltage required can be very low compared to that in normal QWIPs.

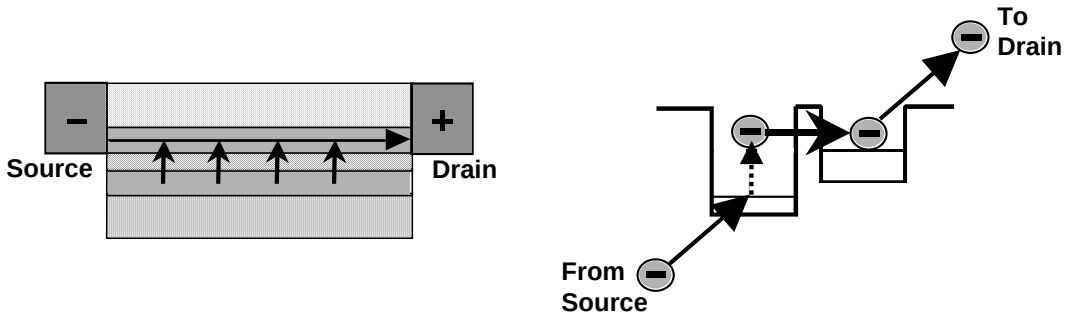

Figure 14: Laterally-biased double quantum well system. On the left we see the conduction path from the source (-) to the drain (+). Electrons in the bottom well absorb a photon and then tunnel through the narrow barrier to the other well, where they feel the bias field and are swept out of the detector and collected as photocurrent. On the right is the band structure diagram for this process.

The requirement of independent control of the lateral bias within each well can be eliminated if we include gate biases to control the current flow within each quantum well due to a common lateral bias. (see Fig. 15) In this case, the upper and lower gate voltages deplete the regions shown in the figure, thus forcing current to flow as shown. By varying either the lateral bias, or the vertical gate bias, the wavelength responsivity can be tuned continuously from the LWIR to the VLWIR and beyond.

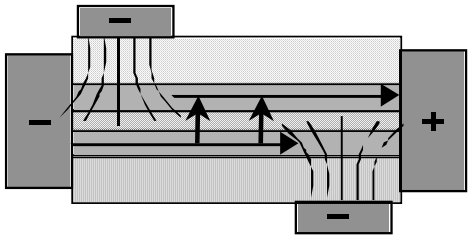

Figure 15: The lateral conduction path when top and bottom gates are biased.

A very important issue that needs to be addressed in GaAs/AlGaAs QWIPs is their relatively low optical coupling efficiency due to an inability to detect normally-incident radiation without a grating (there must be a component of the incident electric field in the confinement direction, i.e., the growth direction). If we could confine the electrons in all three dimensions, these electrons would not be restricted in their coupling to an electromagnetic field. Confinement in three dimensions is called a quantum dot (QD) (of course, atoms are also 3D-confined objects; however, we will restrict our discussion to laboratory-engineered semiconductor structures). The QDs we studied were all fabricated in the Stanski-Krastnov growth mode [8]. Growth of highly mismatched semiconductors leads to the spontaneous formation of islands. The nucleation of the pseudomorphic islands is driven by the strain, and results in the formation of self-organized QDs. Dot formation or coherent islanding occurs to relieve the strain of the lattice mismatch. As the TEM image in Fig. 16 shows, the dots formed with InAs on GaAs are more like pyramids. Their base lengths range from 10 – 20 nm with a height of 2-3 nm. Depending on the growth conditions, different shapes, either pyramidal or lens-like, can be obtained for the islands. Of considerable importance is the fact that the dots are grown epitaxially. Dot densities in the range of $>5x10^{10}$ cm^{-2} are common. Since absorption of the signal photons will occur within these QDs, this density is not very large. To increase the absorption cross section, the dots can be surrounded by a well material, then on that layer a barrier material can be grown, followed by another layer of self-assembled QDs, etc. This new structure is then a multi-layered dots-in-a-well system. (see Fig. 16)

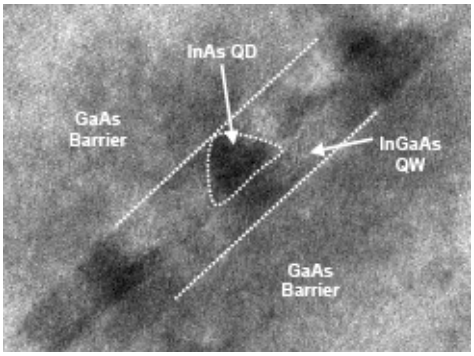

Figure 16: TEM image of quantum dots buried in a quantum well (image taken at the Center for High Technology Materials, University of New Mexico).

The array of self-organized InAs quantum dots are grown near the InAs/GaAs interface by using the strain effect at the interface. As a result, the electrons in the doped GaAs quantum well will sink into the ground state of the InAs QD, which has a much lower energy than the ground state of the quantum well. The deep potential well in the QD effectively reduces the dark current in this structure. When a photon is absorbed by electrons in the QDs, they will be excited to the ground state of the quantum well. For voltage-tunability, the photo-generated carriers in the quantum wells can be transported to the collector using the lateral transport scheme mentioned earlier. We can bury the quantum dots within one of a pair of undoped quantum wells and transport can be accomplished laterally, with the help of tunneling coupling between the wells (see Fig. 17). The key issue for operation in these QDIPs is to guarantee that the non-radiative transition lifetime of electrons in the quantum well ground state back to the QD ground state is longer than the tunneling time between the two quantum wells.

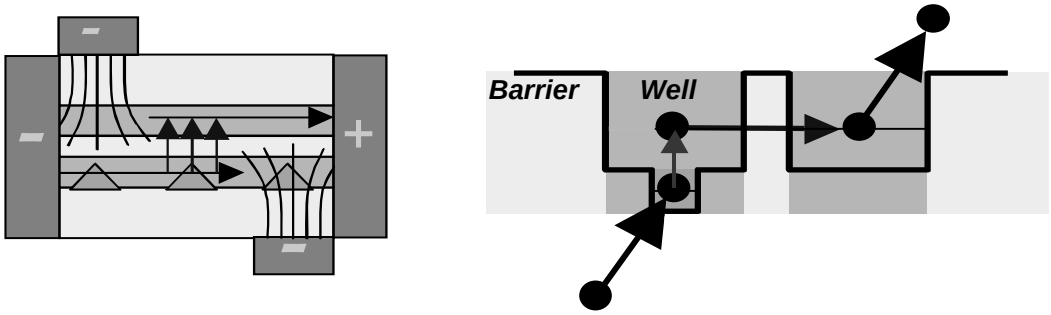

Figure 17: Laterally-biased double quantum well system, with quantum dots (triangles) embedded in the active well. On the left we see the conduction path from the source (-) to the drain (+), with top and bottom biasing gates. On the right is the bandstructure diagram for the transport process described in the text.

4. PHOTOLUMINESCENCE ("LASER") COOLING OF SOLIDS

Infrared photodetectors generally need to be cooled in order to work more efficiently. There are several approaches to cooling solid-state detectors, including mechanical cooling, thermoelectric cooling, thermionic cooling, opto-thermionic cooling, and fluorescent cooling. Some of these cooling concepts provide very attractive possibilities for cryogenics-on-a-chip, either including contacts for a current flow under a bias or excluding contacts by replacing the bias with a resonant optical field.

Solid state cooling will have many advantages for space-based sensing missions. Such a cooler will have no vibration to contend with. It should be free of electronic, magnetic, and electromagnetic noise. With no moving parts, it should have a very long lifetime. The solid-state cooling technologies are accomplished with low-cost materials and manufacturing, and should be highly reliable. A complete solid-state cryocooler with a cubic centimeter of volume (and in some cases, much less than that) seems possible. This extreme miniaturization could lead to cooling a focal plane array, pixel by pixel.

The cooling of a solid via light-induced fluorescence has been of interest for a very long time.[5] This interesting phenomenon involves the excitation of an electron from the valence bandedge to the conduction bandedge by absorbing a pump photon (see Fig. 18). This cool electron quickly becomes hot by gaining thermal energy through ultrafast electron-phonon scattering. After a radiative lifetime, recombination of the hot electron will produce a spontaneous photon with energy higher than that of the pump photon. As a result, the lattice will be cooled due to the loss of thermal energy to the electron. It is only recently that this phenomenon has been observed experimentally. Laser-induced fluorescent cooling of heavy-metal-fluoride glass doped with trivalent ytterbium ions was the first realization of this concept [9].

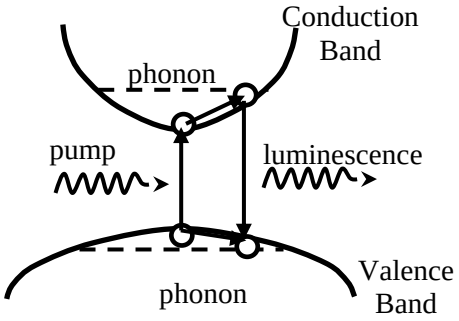

Figure 18: This is a band diagram of the photoluminescence cooling mechanism in semiconductors.

Laser cooling of a semiconductor remains an elusive goal, although it has been pursued for many years. The key question we have tried to answer is: what are the best semiconductor materials and conditions for achieving the greatest laser cooling effect? This requires an accurate *nonlocal* theory on a microscopic level, which directly provides an evolution equation for the lattice temperature by including the dynamical effects. We have developed such a *nonlocal* theory for the laser cooling of semiconductors [10]. By including the effect of the carrier distribution, we were able to uncover the essential physics underlying the phenomenon and we provided important quantitative predictions that can guide experimentalists toward achieving maximum efficiency of laser cooling in the future.

We assumed a weak pump laser first excites electrons from the valence bandedge to the conduction bandedge. The excited carriers instantaneously form a nonequilibrium distribution. It is well known that the quantum kinetics of the scattering of electrons with phonons or other carriers under a weak pump field can only be seen within the time scale of several hundred femtoseconds. Subsequently, ultrafast carrier-phonon and carrier-carrier scattering quickly adjusts the kinetic energies of these excited carriers by taking energy from the lattice. As a result, a quasi-equilibrium Fermi-Dirac distribution of carriers is formed in about 0.1 ps, with an electron temperature determined by the pump-field intensity, pump-photon energy, and lattice temperature. After a few tens of nanoseconds, radiative decay of the excited carriers will begin to affect the electron distribution. The electron temperature will be adiabatically readjusted according to an energy balance between the power-gain density due to optical absorption, the power-loss density due to photoluminescence, and the power-exchange density due to scattering with phonons. At the same time, the lattice temperature will evolve

because of an imbalance between the power loss due to transferring phonon energy to carriers and the slight power gain from the external thermal radiation. Just before the radiative decay occurs, the lattice and the electrons are in thermal equilibrium with an initial temperature which can be determined by solving a semiconductor Bloch equation.

Using our nonlocal theory, we find that the laser-cooling rate is largest for a large bandgap material, a weaker pump-laser field, and a high initial lattice temperature (see Fig. 19). We also find that the laser-cooling power decreases as the lattice cools down.

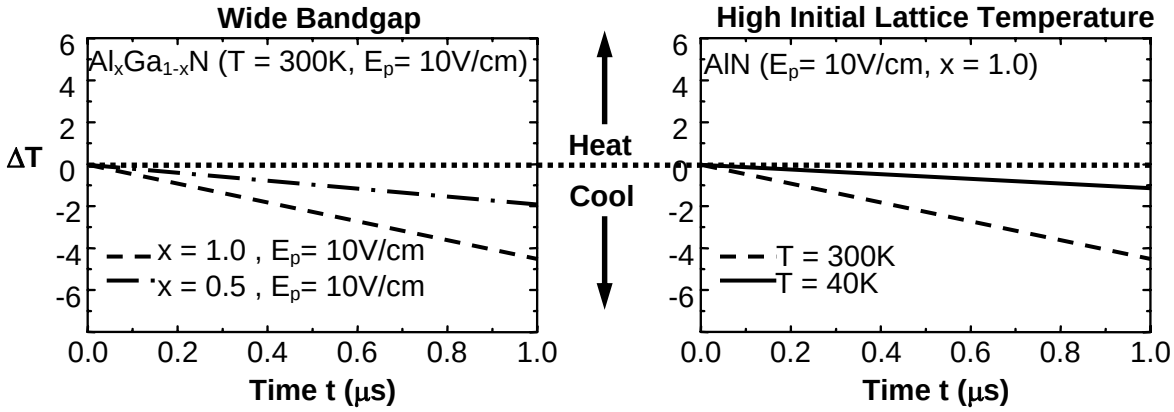

Figure 19: The graph on the left indicates that there is greater cooling for lower pump power and wider bandgap. The graph on the right indicates that there is greater cooling when the initial temperature is higher.

5. SUMMARY

We have described several technologies for use in a monolithically-integrated sensor system for SSA missions. We are working on three parallel schemes for enhancing weak signals using quantum interference and population trapping in quantum-confined structures, plasmon interactions in nano-patterned thin conducting surfaces, and quantum dots in photonic crystal microcavities. We are investigating one possible scheme for tuning the spectral response of a detector using quantum dots buried in quantum wells with a lateral biasing. Finally, we are looking at one possible method for cooling a focal plane pixel by pixel using a solid-state optical cooling scheme. All of these technologies will be compatible with the monolithically-integrated concept.

REFERENCES

1. D. A. Cardimona, M. G. Raymer, and C. R. Stroud, Jr., J. Phys. B **15**, 55 (1982); D. A. Cardimona, M. P. Sharma, and M. A. Ortega, J. Phys. B **22**, 4029 (1989); D. A. Cardimona, Phys. Rev. A **41**, 5016 (1990); D. A. Cardimona and M. P. Sharma, "Method and Apparatus for Field-Induced Transparency Using Laser Radiation," patent number 5,196,097 (1993).
2. D. S. Lee and K. J. Malloy, IEEE J. Quant. Elect. **30**, 85 (1994); Y. Zhao, D. Huang, and C. Wu, Opt. Lett. **19**, 816 (1994); D. Huang and D. A. Cardimona, J. Opt. Soc. Am B **15**, 1578 (1998); D. Huang and D. A. Cardimona, Phys. Rev. A **64**, 013822 (2001); D. A. Cardimona and D. Huang, Phys. Rev. A **65**, 033828 (2002); P. M. Alsing, D. Huang, D. A. Cardimona, and T. Apostolova, Phys. Rev. A **68**, 033804 (2003).
3. S. E. Harris, Phys. Rev. Lett. **62**, 1033 (1989); S. E. Harris, J. E. Field, and A. Imamoglu, Phys. Rev. Lett. **64**, 1107 (1990); S. E. Harris, Phys. Rev. Lett. **72**, 52 (1994).
4. T. W. Ebbesen, H. J. Lezec, H. F. Ghaemi, T. Thio, and P. A. Wolff, Nature (London) **391**, 667 (1998); H. F. Ghaemi, T. Thio, D. E. Grupp, T. W. Ebbesen, and H. J. Lezec, Phys. Rev. B **58**, 6779 (1998).
5. D. H. Huang, Y. Zhu, and S. X. Zhou, J. Phys.: Condens. Matter **1**, 7619 (1989).
6. D. H. Huang, C. Rhodes, P. M. Alsing, and D. A. Cardimona, submitted to JOSA B (2005).
7. M. Soljacic and J. D. Joannopoulos, Nature Materials **3**, 211 (2004).
8. S. Ragavan, P. Rotella, A. Stinz, B. Fuchs, S. Krishna, C. Morath, D. A. Cardimona, and S. W. Kennerly, Appl. Phys. Lett. **81**, 1369 (2002).
9. R. I. Epstein, M. I. Buchwald, B. C. Edwards, T. R. Gosnell, and C. E. Mungan, Nature (London) **37**, 500 (1995).
10. D. H. Huang, T. Apostolova, P. M. Alsing, and D. A. Cardimona, Phys. Rev. B **70**, 033203 (2004).